Enhancement of nonlinear optical properties of $BaTiO_3$ nanoparticles by the addition of silver seeds

Brian G. Yust,[1,*] Neema Razavi,[1] Francisco Pedraza,[1] Zakary Elliott,[1] Andrew T. Tsin,[2] and Dhiraj K. Sardar[1]

[1]*Department of Physics & Astronomy, University of Texas at San Antonio, One UTSA Circle, San Antonio, Tx 78249, USA*

[2]*Department of Biology, University of Texas at San Antonio, One UTSA Circle, San Antonio, Tx 78249, USA*

[*]*bribriwork@gmail.com*

Abstract: Barium titanate ($BaTiO_3$) is an interesting nonlinear material because of its high third order susceptibility. While many nonlinear effects have been extensively studied on the bulk scale, there are still questions regarding the strength of nonlinear effects in nanoparticles. The nonlinear properties of $BaTiO_3$ nanoparticles and nanorods have been studied using the closed aperture z-scan technique. Silver was then grown photochemically on the surface of the $BaTiO_3$ nanoparticles, and it was found that the third order susceptibility increases dramatically.

OCIS codes: (160.4236) Nanomaterials; (190.4720) Optical nonlinearities of condensed matter.

References and links

1. S. Ju, P. R. Watekar, S. Jeong, Y. Kim, and W. T. Han, "Nonlinear optical properties of zinc doped germnao-silicate glass optical fiber," J. Nonlinear Optic. Phys Mat. **19**, 791-799 (2010).
2. P. R. Watekar, S. Moon, A. Lin, S. Ju, and W. T. Han, "Linear and nonlinear optical properties of Si nanoparticles / Er-ions doped optical fiber," J. Lightwave Tech. **27**, 568-575 (2009).
3. J. L. Gu, J. L. Shi, G. J. You, L. M. Xiong, S. X. Qian, Z. L. Hua, and H. R. Chen, "Incorporation of highly dispersed gold nanoparticles into the pore channels of mesoporous silica thin films and their ultrafast nonlinear optical response," Adv. Mat. **17**, 557-560 (2005).
4. H. P. Li, B. Liu, C. H. Kam, Y. L. Lam, W. X. Que, L. M. Gan, C. H. Chew, and G. Q. Xu, "Femtosecond z-scan investigation of nonlinear refraction in surface modified PbS nanoparticles," Opt. Mat. **4**, 321-327 (2000).
5. Y. Wang, C. Y. Lin, A. Nikolaenko, V. Raghunathan, and E. O. Potma, "Four-wave mixing microscopy of nanostructures," Adv. Opt. Phot. **3**, 1-52 (2011).
6. Y. Takeda, O. A. Plaksin, K. Kono, and N. Kishimoto, "Nonlinear optical properties of Cu nanoparticles in various insulators fabricated by negative ion implantation," Surf. And Coat. Tech. **1**, 30-33 (2005).
7. J. Butet, J. Duboisset, G. Bachelier, I. Russier-Antoine, E. Benichou, C. Jonin, and P. F. Brevet, "Optical second harmonic generation of single metallic nanoparticles embedded in a homogenous medium," Nano Lett. **10**, 1717-1721 (2010).
8. P. C. Ray, "Size and shape dependent second order nonlinear optical properties of nanomaterials and its application in biological and chemical sensing," Chem. Rev. **110**, 5332-5365 (2010).
9. J. Butet, I. Russier-Antoine, C. Jonin, N. Lascoux, E. Benichou, and P. F. Brevet, "Sensing with multipolar second harmonic generation from spherical metallic nanoparticles," Nano Lett. **12**, 1697-1701 (2012).
10. C. L. Hsieh, Y. Pu, R. Grange, and D. Psaltis, "Digital phase conjugation of second harmonic radiation emitted by nanoparticles in turbid media," Opt. Exp. **18**, 12283-12290 (2010).
11. L. Tong and J. X. Cheng, "Label-free imaging through nonlinear optical signals," Mat. Today **6**, 264-273 (2011).
12. M. G. Papadopoulos, A. J. Sadlej, and J. Leszczynski, *Non-linear Optical Properties of Matter: From molecules to condensed phases* (Springer, 2006).

13. P. Ren, H. Fan, and X. Wang, "Electrospun nanofibers of ZnO/BaTiO3 heterostructures with enhanced photocatalytic activity," Catal. Comm. **25**, 32-35 (2012).
14. Y. H. Chen and Y. D. Chen, "Kinetic study of Cu(II) adsorption on nanosized BaTiO3 and SrTiO3 photocatalysts," J. Haz. Mat. **1**, 168-173, (2011).
15. N. Venkatram and D. N. Rao, "Nonlinear absorption, scattering and optical limiting studies of CdS nanoparticles," Opt. Exp. **13**, 867-872 (2005).
16. S. Mohapatra, Y. K. Mishra, A. M. Warrier, R. Phillip, S. Sahoo, A. K. Arora, and D. K. Avesthi, "Plasmonic, low-frequency raman, and nonlinear optical-limiting studies in copper-silica nanocomposites," Plasmonics **1**, 25-31 (2012)
17. B. Palpant, M. Rashidi-Huyeh, B. Gallas, S. Chenot, and S. Fisson, "Highly dispersive thermo-optical properties of gold nanoparticles," Appl. Phys. Lett. **90**, 223105 (2007).
18. R. A. Ganeev, M. Baba, A. I. Ryasnyansky, M. Suzuki, and H. Kuroda, "Characterization of optical and nonlinear optical properties of silver nanoparticles prepared by laser ablation in various liquids," Opt. Comm. **240**, 437-448 (2004).
19. R. de Nalda, R. del Coso, J. Requejo-Isidro, J. Olivares, A. Suarez-Garcia, J. Solis, and C. N. Afonso, "Limits to the determination of the nonlinear refractive index by the z-scan method," J. Opt. Soc. Am. B **19**, 289-296 (2002).
20. A. Gnoli, L. Razzari, and M. Righini, "Z-scan measurements using high repetition rate lasers: how to manage thermal effects," Opt. Exp. 13, 7976-7981 (2005).
21. R. A, Ganeev, M. Suzuki, M. Baba, M. Ichihara, and H. Kuroda, "Low- and high-order nonlinear optical properties of BaTiO3 and SrTiO3 nanparticles," J. Opt. Soc. Am. B **25**, 325-333 (2008).
22. P. K. Dutta and J. R. Gregg, "Hydrothermal synthesis of tetragonal barium titanate (BaTiO3)," Chem. Mater. **4**, 843-846 (1992).
23. M. Wu, J. Long, G. Wang, A. Huang, Y. Luo, S. Feng, and R. Xu, "Hydrothermal synthesis of tetragonal barium titanate from barium hydroxide and titanium dioxide under moderate conditions," J. Am. Chem. Soc. **82**, 3254-3256 (1999).
24. S. G. Kwon, K. Choi, and B. Kim, "Solvothermal synthesis of nano-sized tetragonal barium titanate powders," Mat. Lett. **60**, 979-982 (2006).
25. J. Giocondi and G. Rohrer, "Spatially selective photochemical reduction of silver on the surface of ferroelectric barium titanate," Chem. Mater. **13**, 241-242 (2001).
26. R. Ganeev, G. Boltaev, R. Tugushev, and T. Usmanov, "Nonlinear optical absorption and refraction in Ru, Pd, and Au nanoparticle suspensions," Appl. Phys. B **3**, 571-576, (2010).
27. M. Shik-Bahae, "Sensitive measurement of optical nonlinearities using a single beam," J. of Quantum Electronics **26**, 760-769, (1990).
28. M. H. Majiles Ara, Z. Dehghani, R. Sahraei, and G. Nabiyouni, "Non-linear optical properties of silver nanoparticles prepared by hydrogen reduction method," Opt. Comm. **283**, 1650-1653 (2010).
29. G. Yang, Z. Youhua, H. Long, Y. Li, and Y. Yang, "Optical nonlinearities in Ag/BaTiO3 multi-layer nanocomposite films," Thin Solid Films **515**, 20-21 (2007).
30. R. Karimzadeh and N. Mansour, "The effect of concentration on the thermo-optical properties of colloidal silver nanoparticles," Opt. & Las. Tech. **42**, 783-789 (2010).
31. J. P. Gordon, R. C. Leite, R. S. Moore, S. P. Porto, and J. R. Whinnery, "Long-transient effects in lasers with inserted liquid samples," J. Appl. Phys. **36**, 3-8 (1965).
32. F. L. S. Cuppo, A. M. F. Neto, and S. L. Gomez, "Thermal-lens model compared with the Sheik-Bahae formalism in interpreting z-scan experiments on lyotropic liquid crystals," J. Opt. Soc. Am. B **19**, 1342-1348 (2002).
33. M. Falconieri, "Thermo-optical effects in z-scan measurements using high-repetition-rate lasers," J. Opt. A: Pure Appl. Opt. **1**, 662-667 (1999).
34. G. Yang, W. Wang, Y. Zhou, H. Lu, G. Yang, and Z. Chen, "Linear and nonlinear optical properties of Ag nanocluster/BaTiO3 composite films," Appl. Phys. Lett. **81**, 3969-3971 (2002).
35. Y. Pu, R. Grange, C. L. Hsieh, and D. Psaltis, "Nonlinear optical properties of core-shell nanocavities for enhanced second-harmonic generation," Phys. Rev. Lett. **104**, 207402 (2010).

1. Introduction

Nonlinear optical materials have been studied for many years and have been utilized in a wide range of applications. With the increasing use of and interest in nanomaterials, it is important that these phenomena be explored in the nanoscale regime in order to better understand the interactions of matter with light on this level. In particular, nonlinear optical nanomaterials have the potential to enhance and extend techniques and devices in the areas of communications [1, 2, 3], optical devices [4, 5, 6], biosensors [7, 8, 9], and imaging [7, 10, 11]. While many nonlinear effects were once thought to only occur on the bulk scale, it has

been shown that some nonlinear effects, such as four wave mixing and harmonic generation in nanocrystals, can still occur at the nanoscale [5, 10, 12]. Nanomaterials with large nonlinear responses can be used as contrast agents in nonlinear microscopy [7, 9, 11], as biosensors [7, 8, 9], photocatalysts [13, 14], optical limiters [15, 16], and in photonic devices [4, 5, 6]. In order to quantify the nonlinear optical properties of nanomaterials, the closed aperture z-scan technique was used on samples of $BaTiO_3$ and silver seeded $BaTiO_3$ ($Ag@BaTiO_3$) nanoparticles in solution. While many nonlinear effects are driven through higher energy density pulses, especially in metal nanomaterials, the nonlinear response of $BaTiO_3$ and $Ag@BaTiO_3$ nanoparticles occurs in both the continuous wave and pulsed regimes. In this work, we focus on the nonlinear properties of $BaTiO_3$ nanoparticles in the continuous wave regime and the enhancement of these properties with the addition of silver seeds. While the nonlinear properties are likely dominated by the thermo-optic nonlinearities under continuous wave and longer pulse illumination [17, 18, 19], measuring the properties with the z-scan yields the total effective nonlinear refractive indices and absorption, making it difficult to separate purely optical effects from thermal effects [20]. With the applications for these particles potentially using either type of laser source, the nonlinear response of these particles needs to be investigated.

2. Materials

Barium titanate ($BaTiO_3$) is a perovskite crystal with a high third order susceptibility when in the tetragonal phase, so it is well suited for nonlinear imaging techniques, such as third harmonic generation and optical phase conjugation [21]. $BaTiO_3$ nanoparticles (NPs) were fabricated with average diameters of 200 nm and 500 nm through either the hydrothermal or solvothermal synthesis method (Fig. 1) [22 – 24]. In a typical synthesis, barium chloride or barium hydroxide was used as the barium source. This was mixed with titanium dioxide in an aqueous or water/ethanol solution with sodium and potassium hydroxide, sealed in a steel autoclave, and heated at 190 °C for 12 – 48 hours. All chemicals used were of 99% purity and were purchased from Sigma Aldrich. Also, $BaTiO_3$ NPs were purchased from NanoAmour of Houston, Tx to provide a standard for crystallinity and optical properties. In addition, $BaTiO_3$ nanorods with diameters of 50 nm and average lengths of 250 nm and Ba_2YbF_7 nanoparticles were also fabricated using the hydrothermal method to provide secondary structures to compare with the nonlinear properties of the larger $BaTiO_3$ particles (Figs. 2, 3).

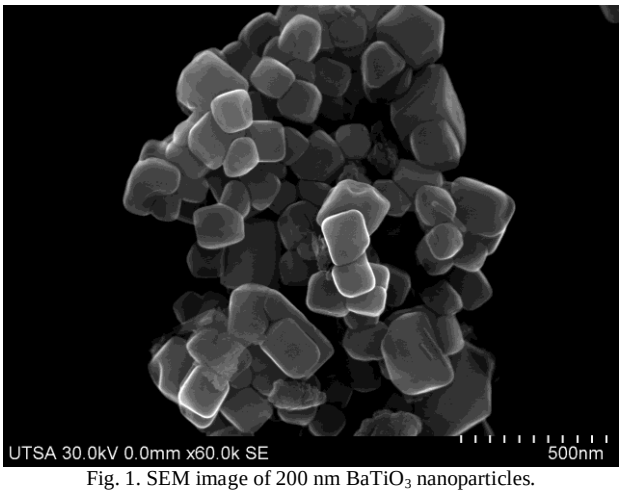

Fig. 1. SEM image of 200 nm $BaTiO_3$ nanoparticles.

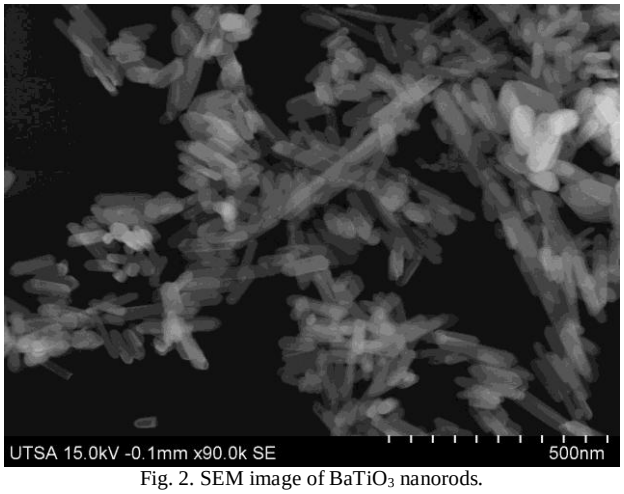

Fig. 2. SEM image of $BaTiO_3$ nanorods.

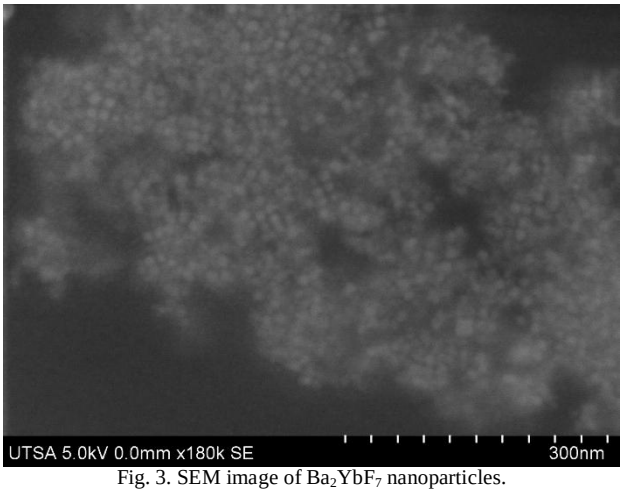

Fig. 3. SEM image of Ba_2YbF_7 nanoparticles.

Silver was seeded onto the 200 nm and 500 nm $BaTiO_3$ nanoparticles by photoreduction of silver nitrate in solution with $BaTiO_3$ and polyvinylpyrrolidone (PVP) which mediated the growth of silver seeds on the surface as opposed to forming silver particles separately in the solution. In a typical silver deposition, 0.3 g of $BaTiO_3$ nanoparticles were suspended in a half ethanol, half water solution with 0.3 g of PVP and 0.6 g of $AgNO_3$. This solution was exposed to visible illumination from a tungsten-halogen lamp at 200 W for 1.5 hours while under vigorous stirring. The size of the silver seeds on the surface is directly related to the time of exposure during photochemical reduction, and 1.5 hours was chosen so that the silver seeds growing on the NPs did not become so large that they began to detach from the $BaTiO_3$. Figs. 4 and 5 illustrate the Ag seeds grown by photochemical deposition on the facets of $BaTiO_3$. Those facets with the positive ends of the polarization vector directed toward the surface preferentially grow the Ag seeds, as was found in a previous study of $BaTiO_3$ bulk samples [25].

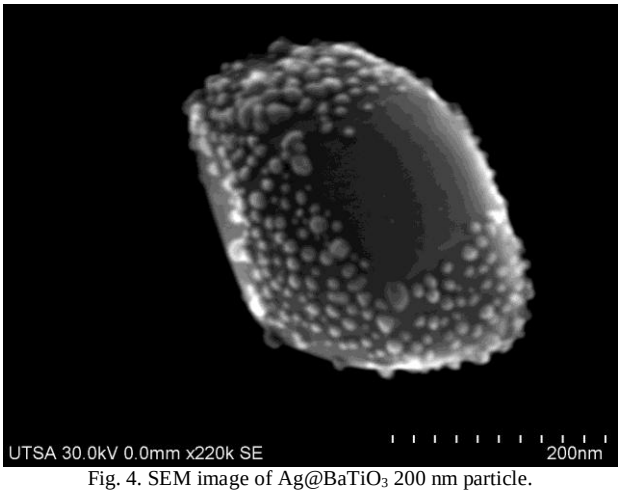

Fig. 4. SEM image of $Ag@BaTiO_3$ 200 nm particle.

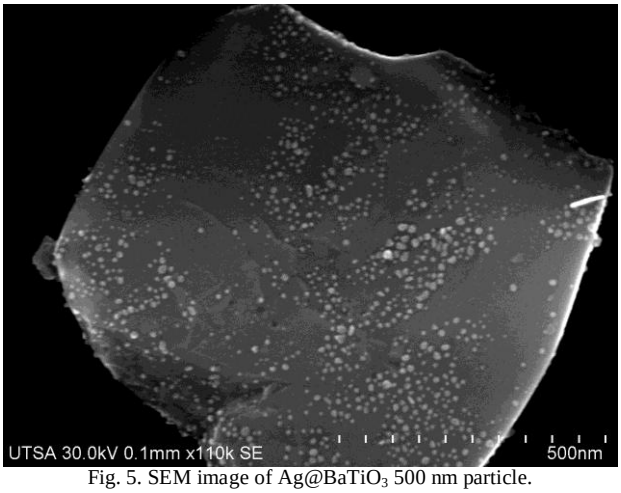

Fig. 5. SEM image of $Ag@BaTiO_3$ 500 nm particle.

3. Experimental setup

The nonlinear properties of nanoparticles were investigated using the well known closed aperture z-scan technique [21]. In this setup, a Spectraphysics DPSS laser (λ = 532 nm) was focused through a lens with f = 7.3 cm with a detector in the far field with a small aperture (S << 1) aligned to the center of the beam (Fig. 1). A translational stage was placed such that solutions containing the nanoparticles, placed within a quartz microcuvette (L = 2 mm), traversed the focal point (Fig. 6).

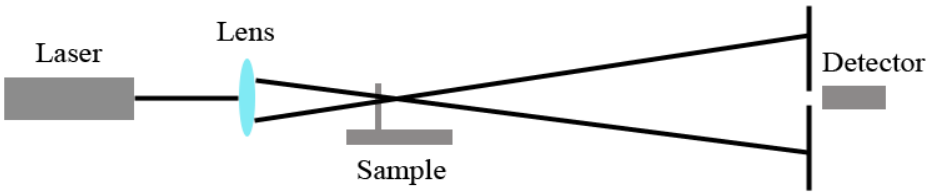

Fig. 6. Experimental setup for closed aperture Z-scan.

Although the nonlinear effects were observed with a continuous wave source, both visually and by measurement, a chopping blade (200 Hz) was placed in the beam pathway, and a lock-in amplifier was added to the setup to increase the signal to noise ratio and stability of the signal. As described in previous work, the nonlinear optical properties can be extracted through fitting plots of the transmittance with the Eq. (1) [21, 26]:

$$T(z) = 1 + \frac{4x}{(x^2+9)(x^2+1)} \mathrm{DF}_0 - \frac{2(x^2+3)}{(x^2+9)(x^2+1)} \mathrm{DY}_0 \quad (1)$$

where $x = z/z_0$, and $z_0 = k\omega_0^2/2$ is the diffraction length, $k = 2\pi/\lambda$, ω_0 is the beam waist radius, $\Delta\Phi_0 = k\gamma I_0 L_{eff}$ is the phase change due to the nonlinear refractive index, γ, $\Delta\Psi_0 = \beta I_0 L_{eff}/2$ is the phase change due to nonlinear absorption, β, $I_0 = \frac{2P_{in}}{\pi\omega_0^2}$ is the irradiance at the focal point of the lens, and $L_{eff} = (1-e^{-\alpha L})/\alpha$ is the effective length of the sample with α being the linear absorption coefficient. With the z-scan setup used, the irradiance at the focal point of the lens, I_0, was calculated to be 0.116 MW/cm^2. The original peak-to-valley measurement first introduced by Sheik-Bahae, et. al. was also used to calculate the phase change by the following Eq. (2) [27, 28]:

$$\Delta T_{PV} = 0.406(1-S)^{0.25} \left|\Delta\Phi_0\right| \quad (2)$$

where S is the linear transmittance of the aperture. From the nonlinear refractive index and nonlinear absorption, the real and imaginary parts of the third order susceptibility for the solutions may be obtained with the relations [29]:

$$\mathrm{Re}\left[\chi^3\right](esu) = cn_0^2 g(m^2/W)/120p^2 \quad (3)$$

$$\mathrm{Im}\left[\chi^3\right](esu) = c\lambda n_0^2 \beta(m/W)/480\pi \quad (4).$$

Under the condition of cw laser illumination, it has been noted that the Sheik-Bahae formalism is not the most accurate description since it does not take into account heat diffusion within the samples and nonlocal interaction of the laser beam with the nanoparticles [30, 31, 32]. As such, the formalism developed by Cuppo, et al. which is based on a thermal lens model is also considered, where the transmittance can be described by Eq. 5 [31, 32]:

$$T(z) = \left[1 + \frac{2x}{(1+x^2)} \mathrm{DF}_0 + \frac{1}{(1+x^2)} \mathrm{DF}_0^2\right]^{-1} \quad (5)$$

Falconieri also addressed the issue of calculating thermal nonlinearities from z-scan measurements by using an aberrant thermal lens model, where the transmission can be described by Eq. 6 [33]:

$$T(z) = \left[1 + \frac{\mathrm{DF}_0}{2} \tan^{-1}\left(\frac{2x}{1+x^2}\right)\right]^2 \quad (6)$$

From Eqs. 5 and 6, the nonlinear index of refraction due to thermal effects can be calculated using the same relation found in the definition of the phase change. Although the measurements were made under cw illumination, and thermo-optical effects are expected to dominate, the measurements were treated with each of the four formalisms in order to obtain a clearer picture of the properties of Ag@$BaTiO_3$ under these conditions.

4. Results

The z-scan technique was performed multiple times on each of the nanoparticle types separately prepared in an aqueous solution; examples of the results for each type of nanoparticle are given in Figs. 7 – 12. The error bars represent the standard deviation between the high and low values obtained for each point along the z-scan. Nonlinear fitting of the previously described Eq. (1) was conducted using the phase changes due to the nonlinear refractive index and nonlinear absorption as the fitting parameters. The distinctive peak-to-valley shape of the closed aperture z-scan is a clear indication of third order nonlinear processes, which was present in each of the samples. The nonlinear refractive index and absorption was calculated for each of the as prepared samples and can be found in Table 1.

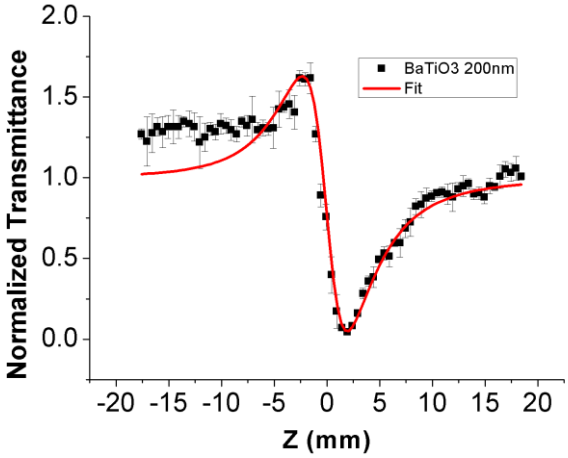

Fig. 7. Z-scan of 200 nm $BaTiO_3$ nanoparticles in solution.

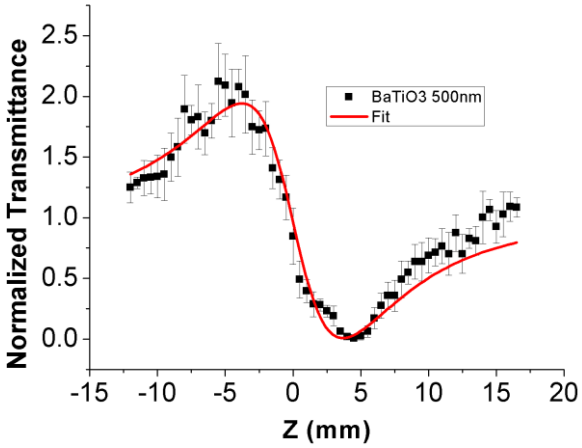

Fig. 8. Z-scan of 500 nm $BaTiO_3$ nanoparticles in solution.

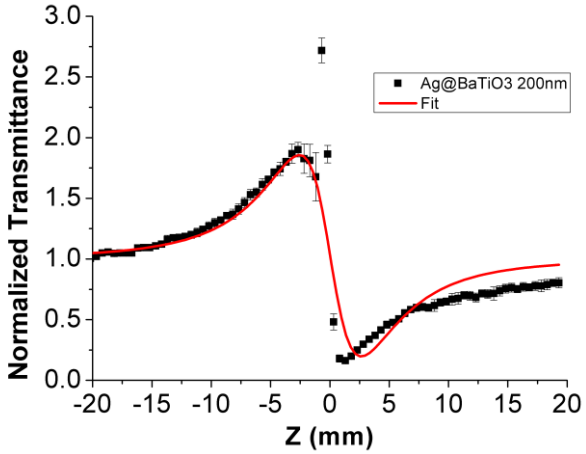

Fig. 9. Z-scan of 200 nm $Ag@BaTiO_3$ nanoparticles in solution.

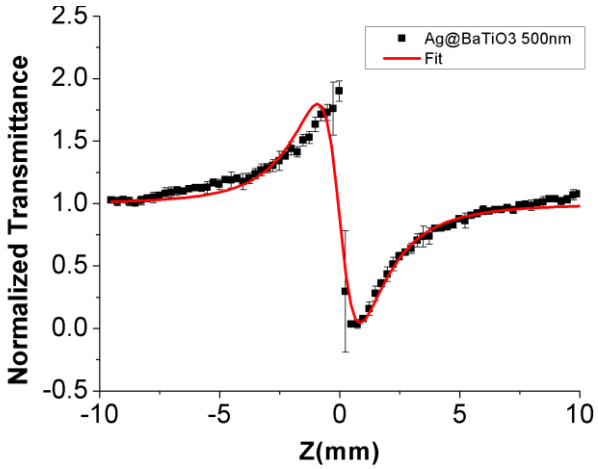

Fig. 10. Z-scan of 500 nm $Ag@BaTiO_3$ nanoparticles in solution.

Table 1. Nonlinear refractive indices, absorptions, and third order susceptibilities of prepared sample solutions calculated by the Sheik-Bahae fitting (SB), peak-to-valley (PV), thermal lens (TL), and aberrant thermal lens (ATL) formalisms.

	SB		PV	TL	ATL
Material	Im χ^3 (10^{-7} esu)	Re χ^3 (10^{-7} esu)	Re χ^3 (10^{-7} esu)		
$Ag@BaTiO_3$ 500 nm	1.60349 ± 0.951	4.06765 ± 0.988	5.32870 ± 2.132	1.06085 ± 0.428	2.56948 ± 0.912
$Ag@BaTiO_3$ 200 nm	0.55597 ± 0.521	1.53869 ± 0.340	4.92555 ± 1.350	1.08935 ± 0.246	2.33154 ± 0.234
500 nm $BaTiO_3$	0.36369 ± 0.091	0.71641 ± 1.114	3.04912 ± 2.142	0.59180 ± 0.360	1.26332 ± 0.699
200 nm $BaTiO_3$	0.21712 ± 0.084	1.01674 ± 0.773	2.79302 ± 1.340	0.38235 ±0.261	0.77149 ± 0.572
250 nm $BaTiO_3$ nanorods	0.22317 ± 0.236	0.38532 ± 0.184	1.29807 ± 0.365	0.77274 ± 0.201	1.27121 ± 0.315
Ba_2YbF_7	0.25137 ± 0.012	0.35598 ± 0.002	1.50247 ± 0.090	0.51984 ± 0.047	1.14818 ± 0.040

The z-scan results for each nanoparticle solution clearly show the peak-to-valley shape which indicates third order nonlinear properties. The nonlinear response from the

nanoparticle solution was clearly visible in the far-field during measurement in the laboratory, demonstrated by a self-focused intense disk when the sample was on the side closer to the lens and laser source and as a self-defocused optical vortex when the sample was on the opposite side of the focal point. As was expected, the tetragonal 500 nm and 200 nm $BaTiO_3$ nanoparticles exhibited higher nonlinear indices of refraction than the smaller, cubic $BaTiO_3$ nanorods. The Ba_2YbF_7 nanoparticles exhibited the lowest third order susceptibility which is likely due to their extremely small size and crystalline structure. Comparing the silver seeded $BaTiO_3$ nanoparticles to those without silver seeds, there is a clear and dramatic increase in the third order susceptibility. Not surprisingly, the 500 nm Ag@ $BaTiO_3$ samples exhibited the largest susceptibility, but it is important to note that even the 200 nm Ag@ $BaTiO_3$ samples had a larger susceptibility than the 500 nm and 200 nm $BaTiO_3$. This enhancement of the nonlinear response is likely due to the silver seeds creating either localized heating around the nanoparticles, increasing the thermo-optical nonlinearities, or by localized electromagnetic field enhancements which allow a polarization to be more easily induced in the nanocrystalline $BaTiO_3$. The results calculated from the Sheik-Bahae formalism were slightly lower than those from the peak-to-valley calculation, although they were still in good agreement. Since it depends on the whole range of values rather than just the maximum and minimum, the nonlinear curve fitting tends to be more accurate which is why it has smaller standard deviations. The results obtained using the thermal lens and aberrant thermal lens formalisms are slightly lower than those obtained using the Sheik-Bahae equations, yet are still in good agreement. It is important to note that within each mathematical treatment, the $Ag@BaTiO_3$ samples continually showed a significant increase in the nonlinear response over the bare $BaTiO_3$ nanoparticles.

The results obtained for the $Ag@BaTiO_3$ samples compare well with those available in the literature with our results being slightly higher than one reference for silver deposited on $BaTiO_3$ thin films, Re $\chi^3 = -2.56*10^{-7}$ esu and Im $\chi^3 = -1.45*10^{-8}$ esu [10], and slightly lower than one for $Ag/BaTiO_3$ nanocomposite thin films, Re $\chi^3 = 8.567*10^{-6}$ esu and Im $\chi^3 = 4.151*10^{-7}$ esu [34]. While these reported results were obtained using nanosecond laser pulses, the role which thermal nonlinearities play in z-scan measurements with different laser sources has been the subject of many papers, such as those by Ganeev and de Nalda, and thermal nonlinearities were determined to be non-negligible even down to nanosecond pulses, especially with a high repetition rate [18, 19]. Given that the mechanisms for the nonlinear properties of our samples and those previously mentioned are very similar, they provide a reasonable measure to compare with our results. In similar nanocomposites of $BaTiO_3$ nanoparticles surrounded by a Au shell, it was shown by Pu, et al., that there was an increase in the second harmonic generation by a factor of 500 when excited near the plasmon resonance of the nanocavity [35]; we expect to see similar results in our own samples when excited near the plasmon resonance of the Ag seeds, and it will be interesting to study these enhancements as a function of the size and plasmon resonance of the Ag seeds.

It should be noted that purely silver nanoparticles were also tested with our z-scan setup; however, accurate measurements could not be obtained since the particles began to fuse and aggregate on the surface of the cuvette as soon as they neared the focal point of the system. Also, the z-scan measurements with particularly large error bars, such as the one near the focal point in Fig. 10, showed an anomalously high point in one of the measurments which therefore skiewed the deviation. However, all other measurements at these points were very close to each other, and the anomalous point was likely due to extra particles moving through the focus of the beam at the exact moment.

5. Conclusion

The nonlinear properties of different types of nanoparticles were investigated using the z-scan technique. It was found that $BaTiO_3$ nanoparticles with the tetragonal crystalline phase still exhibit high third order susceptibilities even down to 200 nm scales, making it a good nanomaterial for use in nanophotonics applications such as nonlinear microscopy and optical phase conjugation. It was then subsequently shown that the addition of silver seeds on the

surface greatly enhances the third order nonlinear properties for these nanoparticles. More importantly, it has been shown for the first time that the nonlinear susceptibilities for these nanomaterials are on the same order as thin films with similar composition. These highly nonlinear nanomaterials may prove most useful as contrast agents, biosensors, and phase conjugate nanomirrors. As such, under the right conditions, such as in counter-propagating four wave mixing, they could produce phase conjugate waves which will retrace their way back to the originating source and could effectively undo scattering effects of turbid media where they are present. This will have profound implications for their use as imaging contrast agents as well as in nanophotonic and biophotonic devices or sensors. Current work is underway to test the biocompatibility of these materials and utilize them as contrast agents, biosensors, and phase conjugate nanomirrors.

Acknowledgements
This research was supported by the National Science Foundation Partnership for Research and Education in Materials (NSF-PREM) Grant No. DMR – 0934218 and by a grant from the National Institute on Minority Health and Health Disparities (G12MD007591) from the National Institutes of Health. The authors would also like to acknowledge the support from NIH-RCMI Grant No. 5G12RR013646-12.